

Electronic Supplementary Material (ESI)

High-throughput screening of transition metal doping and defect engineering on single layer SnS₂ for water splitting hydrogen evolution reaction

Ruixin Xu,^a Tingting Bo,^a Shiqian Cao,^a Nan Mu,^a Yanyu Liu,^{*b} Mingyan Chen^c and Wei Zhou^{*a}

¹Department of Applied Physics, Tianjin Key Laboratory of Low Dimensional Materials Physics and Preparing Technology, School of Science, Tianjin University, Tianjin 300072, P. R. China.

²College of Physics and Materials Science, Tianjin Normal University, Tianjin, 300387, P. R. China.

³Hongzhiwei Technology (Shanghai) Co., Ltd., 1599 Xinjinqiao Road, Pudong, Shanghai, China.

*Corresponding author.

E-mail address: weizhou@tju.edu.cn (Wei Zhou), yylu@tjnu.edu.cn (Yanyu Liu)

Section 1

Table S1 The number of valence electron (θ) and the electronegativity (X_M) of doped

TM atom.

TM atom	θ	X_M	TM atom	θ	X_M
Sc	3	1.36	Y	3	1.22
Ti	4	1.54	Zr	4	1.33
V	5	1.63	Nb	5	1.60
Cr	6	1.66	Mo	6	2.16
Mn	7	1.55	Tc	7	1.90
Fe	8	1.83	Ru	8	2.20
Co	9	1.88	Rh	9	2.28
Ni	10	1.91	Pd	10	2.20
Cu	11	1.90	Ag	11	1.93
Zn	12	1.65	Cd	12	1.69
Sn	4	1.96			

Section 2

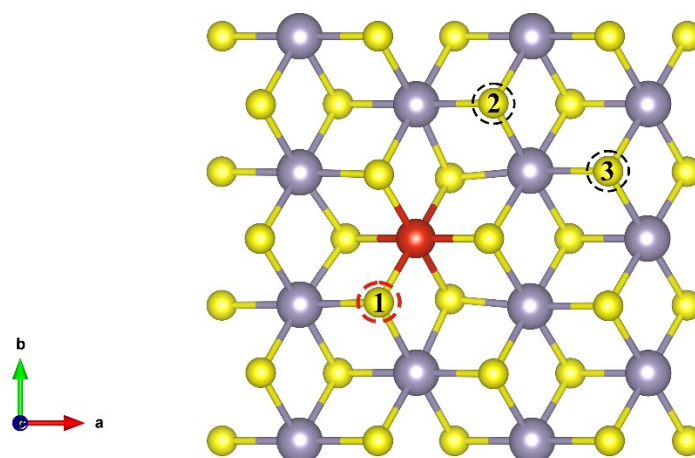


Fig. S1 The top view of three different S sites of TM@SnS₂ nanosheets. The yellow, gray and red balls denote S, Sn and TM atoms, respectively. The red (S1) and black (S2, S3) dotted balls show the S site we chose and other different S sites of H atom adsorption.

Section 3

Table S2 Calculated adsorption energies (E_{ads}) of H atom adsorbed on different S sites of TM@SnS₂ nanosheets.

TM	E_{ads} (eV)			TM	E_{ads} (eV)		
	S1	S2	S3		S1	S2	S3
Sc	-3.25	-3.15	-3.22	Y	-3.26	-3.22	-3.23
Ti	-2.19	-2.05	-2.09	Zr	-1.95	-1.91	-1.95
V	-2.47	-2.32	-2.38	Nb	-2.19	-2.15	-2.13
Cr	-2.87	-2.71	-2.77	Mo	-2.30	-2.26	-2.21
Mn	-2.50	-2.43	-2.41	Tc	-2.61	-2.57	-2.51
Fe	-2.80	-2.71	-2.64	Ru	-2.88	-2.85	-2.74
Co	-3.12	-2.88	-2.94	Rh	-3.13	-3.13	-3.00
Ni	-2.50	-2.05	-2.03	Pd	-2.04	-1.66	-1.62
Cu	-3.31	-2.73	-2.70	Ag	-3.20	-2.62	-2.62
Zn	-3.51	-2.96	-2.99	Cd	-3.30	-2.96	-2.96

Section 4

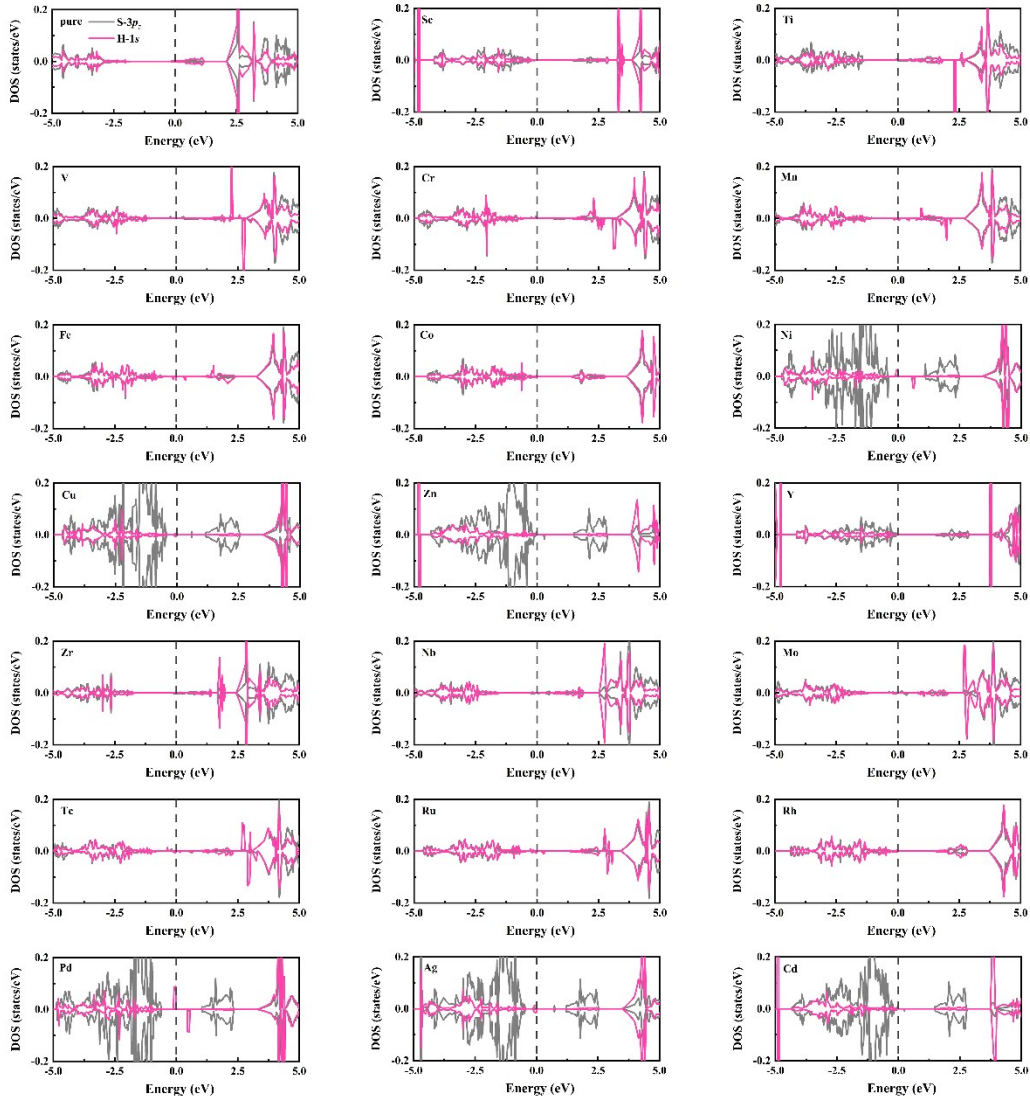


Fig. S2 PDOS of the H-1s and S-3 p_z states in pristine and TM@SnS₂ after H atom adsorption (TM= Sc, Ti, V, Cr, Mn, Fe, Co, Ni, Cu, Zn, Y, Zr, Nb, Mo, Tc, Ru, Rh, Pd, Ag, Cd). The Fermi level is aligned to 0 eV. The gray and pink represent the contributions of S-3 p_z and H-1s states, respectively.

Section 5

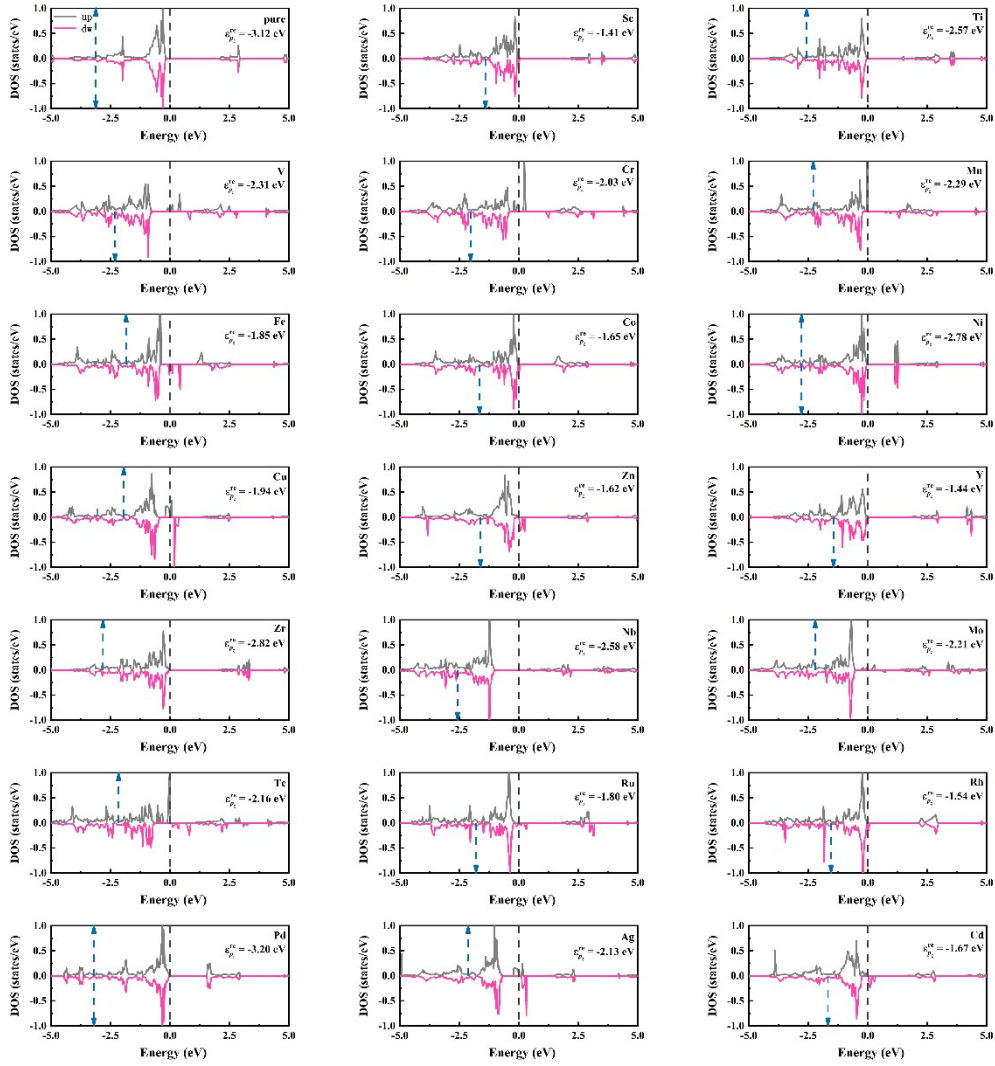


Fig. S3 PDOS of S- $3p_z$ state at active sites in pristine and TM@SnS₂ nanosheets before H atom adsorption. The Fermi level is aligned to 0 eV. The gray and pink represent the contributions of spin up and spin down of S- $3p_z$ states, respectively. The blue arrow shows the position of $\varepsilon(p_z)^{re}$.

Section 6

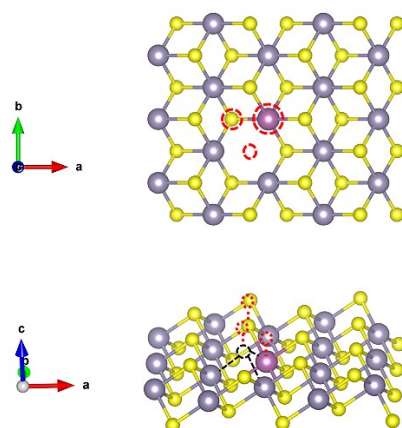


Fig. S4 The top and side views of three adsorption configurations: TM-top site, S-top site and hollow site. The yellow, gray and purple balls denote S, Sn and TM atoms, respectively. The black and pink dotted ball shows S vacancy site and adsorption sites of H atom.

Section 7

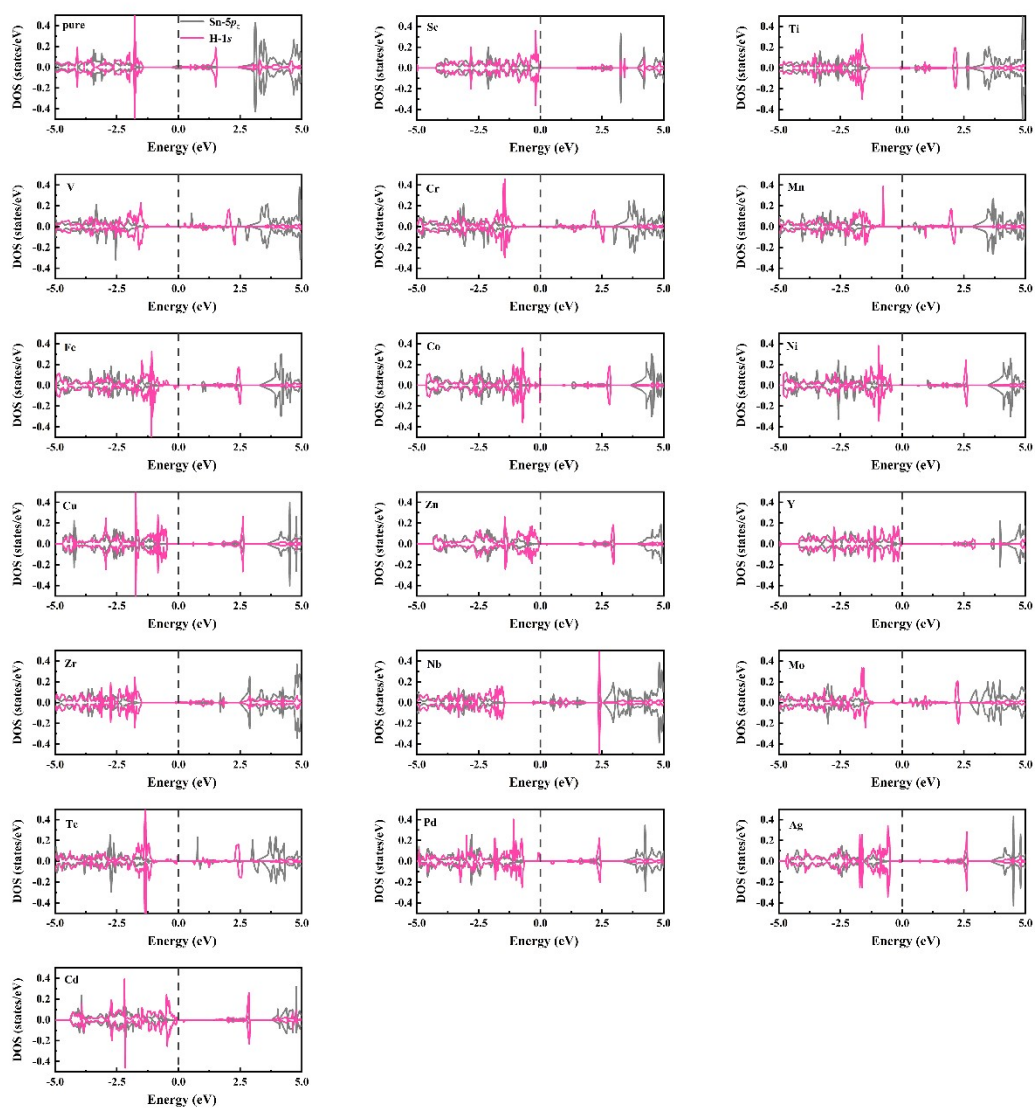


Fig. S5 PDOS of the H-1s and Sn-5p_z states in pristine and TM@V_{s,hollow}-SnS₂ after H atom adsorption. The gray and pink represent the contributions of Sn-5p_z and H-1s states, respectively.

Section 8

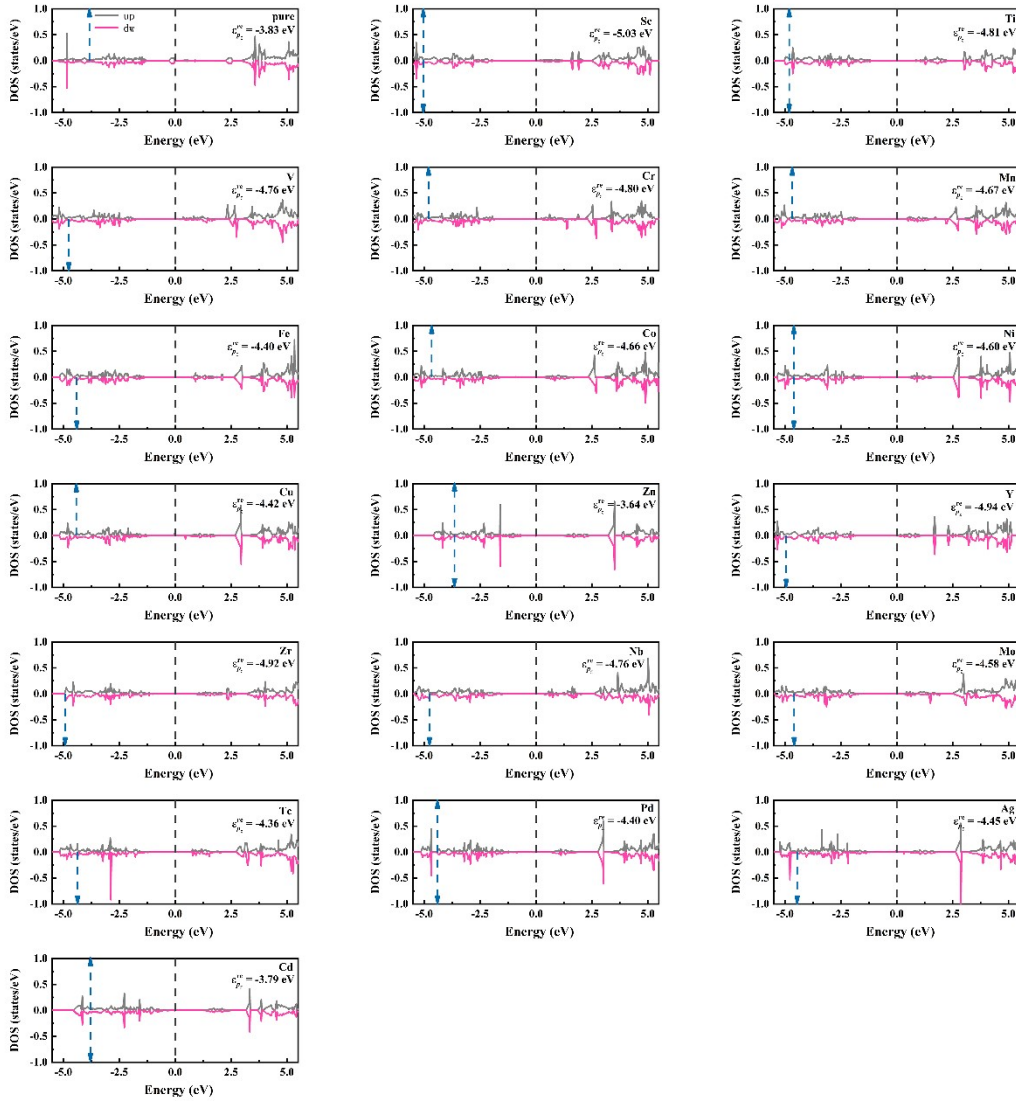


Fig. S6 PDOS of Sn- $5p_z$ state at active sites in pristine and TM@V_{s, hollow}-SnS₂ before H atom adsorption. The gray and pink represent the contributions of spin up and spin down of Sn- $5p_z$ states, respectively. The blue arrow shows the position of $\varepsilon(p_z)^{re}$.

Section 9

Table S3 Relative changes in TM-S ($\Delta d_{TM-S}/d_{TM-S}$) and nearest-neighbors Sn-S ($\Delta d_{Sn-S}/d_{Sn-S}$) bond lengths upon H adsorption at the top of S atom in the basal plane; the distance between the S atom (adsorption site) and the adsorbed H atom (d_{S-H}) in the TM@SnS₂ nanosheets.

TM dopant	$\Delta d_{TM-S}/d_{TM-S}$ (%)	$\Delta d_{Sn1-S}/d_{Sn1-S}$ (%)	$\Delta d_{Sn2-S}/d_{Sn2-S}$ (%)	d_{H-S} (Å)
pure	+5.06	+5.31	+5.06	1.354
Sc	+3.97	+5.37	+5.10	1.352
V	+11.73	+1.60	+1.53	1.355
Mn	+6.01	+2.99	+3.19	1.356
Co	-2.51	+4.95	+5.47	1.358
Ni	+34.80	+2.87	+2.61	1.358
Tc	+6.53	+2.42	+2.44	1.356

Section 10

Table S4 The difference of Bader charge of TM atom and its neighbor S atoms, adsorbed H atom in TM@SnS₂ before and after H atom adsorption.

TM dopant	S1	S2	S3	S4	S5	active site S6	TM	H
pure	0.01	-0.01	-0.01	0.01	0	-0.27	0.02	-0.08
Sc	0.03	0.02	0.02	0.04	0	-0.28	-0.01	-0.08
V	0.02	0.03	0.03	0.03	0.03	-0.26	0.05	-0.08
Mn	0.02	0	0.01	0.02	0	-0.22	0.05	-0.10
Co	0.02	0.01	0.01	0.02	0	-0.20	0.04	-0.10
Ni	0.03	0.03	0.04	0.03	0.02	-0.16	0.01	-0.08
Tc	0.04	-0.03	-0.02	0.05	-0.02	-0.24	0.07	-0.06

Section 11

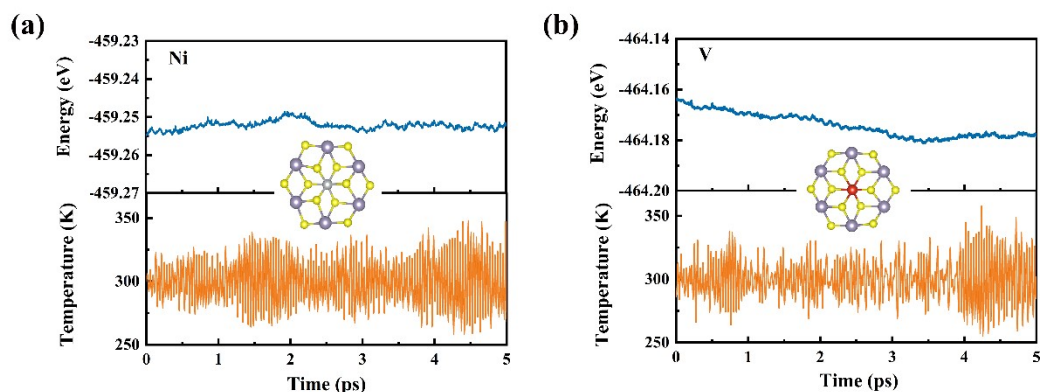


Fig. S7 Variations of energy and temperature of Ni and V@SnS₂ nanosheets against the AIMD simulation time. The insets denote the top view of V, Ni@SnS₂ nanosheets after AIMD simulation lasting for 5 ps at $T=300$ K. It was found that their crystal structures do not present obvious distortion, implying the dynamic stability of these doped nanosheets.

Section 12

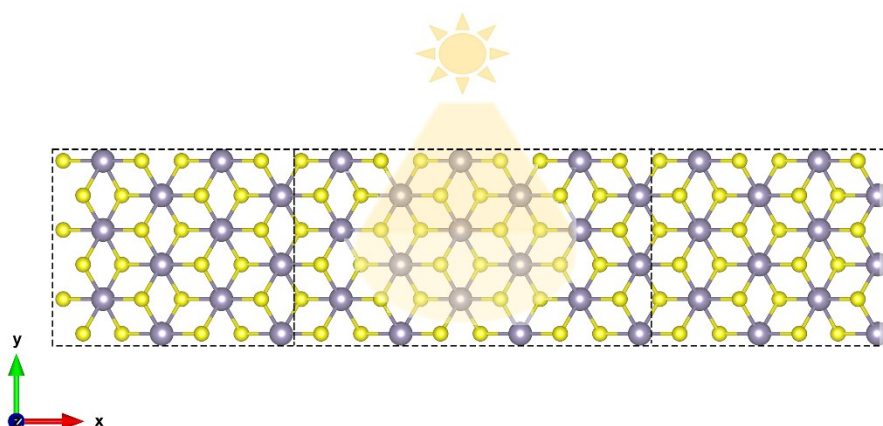


Fig. S8 The schematic diagram of the device model.

Section 13

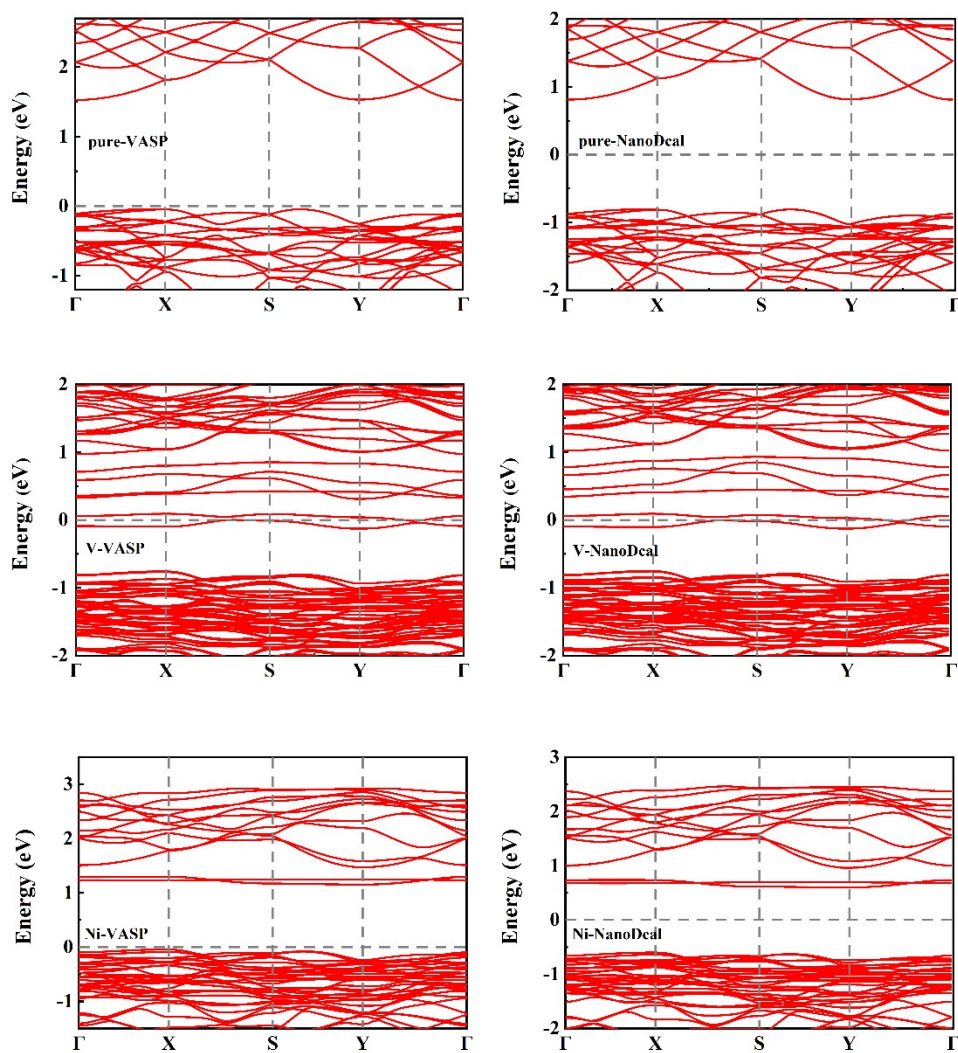


Fig. S9 Calculated band structure of pure, V, Ni@SnS₂ nanosheets by VASP and NanoDcal.

Section 14

The calculation formula of photocurrent^{1,2}.

For linearly polarized light, the photocurrent injected into the left electrode can be written as,

$$J_L^{(ph)} = \frac{ie}{h} \int \left\{ \cos^2 \theta \text{Tr} \left\{ \Gamma_L \left[G_1^{<(ph)} + f_L \left(G_1^{>(ph)} - G_1^{<(ph)} \right) \right] \right\} \right. \quad (1)$$

$$\left. + \sin^2 \theta \text{Tr} \left\{ \Gamma_L \left[G_2^{<(ph)} + f_L \left(G_2^{>(ph)} - G_2^{<(ph)} \right) \right] \right\} \right. \\ \left. + \sin^2 \theta (2\theta) 2 \text{Tr} \left\{ \Gamma_L \left[G_3^{<(ph)} + f_L \left(G_3^{>(ph)} - G_3^{<(ph)} \right) \right] \right\} \right\} dE$$

where

$$G_1^{>(<)}^{ph} = \sum_{\alpha, \beta = x, y, z} C_0 N G_0^r e_{1\alpha} p_\alpha^\dagger G_0^{>(<)} e_{1\beta} p_\beta G_0^a \quad (2)$$

$$G_2^{>(<)}^{ph} = \sum_{\alpha, \beta = x, y, z} C_0 N G_0^r e_{2\alpha} p_\alpha^\dagger G_0^{>(<)} e_{2\beta} p_\beta G_0^a \quad (3)$$

$$G_3^{>(<)}^{ph} = \sum_{\alpha, \beta = x, y, z} \sum_{j=1,2} C_0 N \left(e_{j\alpha} p_\alpha^\dagger G_0^{>(<)} e_{j\beta} p_\beta G_0^a \right) \quad (4)$$

where, $G_{1,2,3}^{>(<)}^{ph}$ are greater than green number and less than green function with the interaction between photon and electron, $G_0^{>(<)}$ is greater than and less than Green's function without photon-electron interaction. Γ_L denotes the line width function of the left electrode. f_L is the Fermi-Dirac distribution function of the left electrode. m stands for net electron mass. I_ω is the photon flux, defined as the number of photons per unit area per unit time. ω is the photon frequency. N represents the number of photons. μ_r , C and ε_r are relative magnetic susceptibility, the speed of light and relative permittivity respectively. ε is the dielectric constant. G_0^a and G_0^r are advanced green's functions and delayed Green's functions respectively. p_α^\dagger and p_β represent the components of the

electron momentum in cartesian coordinates. $e_{1\alpha}, e_{2\alpha}, e_{1\beta}, e_{2\beta}$ sent the unit vector in the Cartesian coordinate system. For linearly polarized light, $\hat{e} = \cos\theta\hat{e}_1 + \sin\theta\hat{e}_2$, where θ is the angle of polarization with respect to vector \hat{e}_1 , and \hat{e}_1, \hat{e}_2 represent the unit vector. To make the calculation of photocurrent more convenient, the current is normalized, and the optical response function is written as:

$$R = \frac{J_L^{(ph)}}{eI_\omega} \quad (5)$$

References

1. J. Chen, Y. Hu and H. Guo, *Phys. Rev. B*, 2012, **85**.
2. L. Zhang, K. Gong, J. Chen, L. Liu, Y. Zhu, D. Xiao and H. Guo, *Phys. Rev. B*, 2014, **90**.